ELSEVIER

Journal of Chromatography A, 925 (2001) 251–263

JOURNAL OF CHROMATOGRAPHY A

www.elsevier.com/locate/chroma

Reversed-phase electrochromatography of amino acids and peptides using porous polymer monoliths

Renée Shediac, Sarah M. Ngola[1], Daniel J. Throckmorton, Deon S. Anex[2], Timothy J. Shepodd, Anup K. Singh*

Chemical & Radiation Detection Laboratories, Sandia National Laboratories, Livermore, CA 94551-0969, USA

Received 20 March 2001; received in revised form 29 May 2001; accepted 6 June 2001

Abstract

Efficient and rapid separation of minute levels of amino acids and bioactive peptides is of significant importance in the emerging field of proteomics as well as in the clinical and pharmaceutical arena. We have developed novel UV-initiated acrylate-based porous polymer monoliths as stationary phases for capillary- and chip-electrochromatography of cationic, anionic, and neutral amino acids and peptides, followed by absorbance or laser-induced fluorescence detection. The rigid monoliths are cast-to-shape and are tunable for charge and hydrophobicity. For separations at low pH, monoliths containing quaternary amine moieties were used to achieve high electroosmotic flow, and for high pH separations monoliths with acidic sulfonic acid groups were employed. Efficient and reproducible separations of phenylthiohydantoin-labeled amino acids, native peptides, and amino acids and peptides labeled with naphthalene-2,3-dicarboxaldehyde (NDA) were achieved using both negatively- and positively-charged polymer monoliths in capillaries. Separation efficiencies in the range of 65 000–371 000 plates/m were obtained with capillary electrochromatography. Buffer composition and the degree of column hydrophobicity were studied systematically to optimize separations. The monoliths were also cast in the microchannels of glass chips and electrochromatographic separation followed by laser-induced fluorescence detection of three NDA-labeled bioactive peptides was obtained.

Keywords: Electrochromatography; Monolithic columns; Stationary phases, electrochromatography; Derivatization, electrochromatography; Chip technology; Amino acids; Peptides

1. Introduction

Achieving high-resolution separations of amino acids and peptides has important implications for amino acid analysis, peptide sequencing, protein structure determination, and the rapidly emerging field of proteomics. High-performance liquid chromatography (HPLC) has been the method of choice for separation of biological molecules [1,2] but recently significant progress has been made towards employing capillary electrochromatography (CEC) for separation of proteins [3–7], peptides [3,5,8,9], and amino acids [10–13]. Electrochromatography, a powerful technique that combines the strengths of

*Corresponding author. Mailstop 9951, Sandia National Laboratories, Livermore, CA 94551-0969, USA. Tel.: +1-925-294-1260; fax: +1-925-294-3020.

E-mail address: aksingh@sandia.gov (A.K. Singh).

[1]Present address: LumiCyte, Fremont, CA 94538-6532, USA.

[2]Present address: Eksigent Technologies, Livermore, CA 94550, USA.

0021-9673/01/$ – see front matter
PII: S0021-9673(01)01036-6

capillary zone electrophoresis (CZE) and liquid chromatography, is especially attractive for development of portable analysis systems as it is readily amenable to miniaturization. Traditionally, CEC has been performed using fused-silica capillaries packed with spherical silica particles. There are a number of drawbacks associated with packed capillaries, such as the time and effort required for packing, the necessity for frits, and the potential leakage of particles. Packing of channels in a chip is considerably more tedious and requires microfabrication of geometrical features to serve as frits. In contrast, in situ casting of polymer monoliths in capillaries and microchannels reproducibly affords relatively uniform packed beds, therefore eliminating the difficulties associated with packing silica beads and the need for retaining frits. The availability of a wide range of monomers enables critical stationary phase properties such as charge and hydrophobicity to be easily tuned to meet the specific demands of separating many types of analytes. In situ polymerization can be thermal- or photo-initiated but the latter has been reported to produce columns with higher separation efficiencies and is also more suitable for casting patterned monoliths in microfabricated channels [8]. In the last few years, owing to their unique properties, porous polymer monoliths have been utilized as stationary phases for CEC, pioneered by Hjertén and coworkers [4,14], and later modified by several groups including Fréchet and coworkers [15–20], Novotny [21], and Horváth and coworkers [7,22,23]. Acrylate-based polymer monoliths developed in our laboratory [24] require a very short (5–20 min) cure time under UV irradiation and support sufficient EOF as cast (no pressure flushing is necessary), making them especially suitable for chip-based application. These materials have reproducibly demonstrated high efficiencies (>150 000 plates/m) for CEC separation of neutral aromatic compounds but their applicability as separation media for charged analytes has not been investigated in detail.

To date, CEC has been predominantly applied to separation of neutral molecules where electrophoretic mobility is not a factor. In CEC of charged molecules, the separation mechanism couples two simultaneous phenomena — the electrophoretic migration of analytes, and the differential partitioning of analytes in stationary and mobile phases. Since biological molecules such as peptides and proteins have multiple ionizable groups that are charged and exhibit varying degrees of polarity, CEC is a potentially powerful tool for their biochemical analysis. In this work, we report the separation of neutral, cationic, and anionic amino acids and peptides by CEC using acrylate-based UV-initiated hydrophobic porous polymers as monolithic stationary phases. Depending on the pH of the mobile phase and the nature of the analytes, either cationic or anionic groups were incorporated into the monoliths for generation of EOF. Selectivity was easily tuned by manipulating the degree of polymer hydrophobicity. Chip electrochromatography using in situ cast polymer monoliths was employed to separate three fluorescently-labeled bioactive peptides, demonstrating the applicability of these materials as separation media in microfluidic devices.

2. Experimental

2.1. Apparatus

Polymerization was performed in a Spectrolinker XL-1500 UV crosslinker (Westbury, NY, USA) operated at 365 nm, according to a procedure described elsewhere [24]. CEC, capillary electrophoresis (CE), and chip electrochromatography experiments were performed using a Bertan 30 kV current-limited, adjustable d.c. power supply (Hicksville, NY, USA). UV absorbance was monitored using a Linear 200 detector (San Jose, CA, USA) set at 214 nm. Laser-induced fluorescence (LIF) detection was performed using a 413 nm krypton ion laser (Coherent, Santa Clara, CA, USA). A chip station was built in the laboratory, and both capillary and chip systems were enclosed in a Plexiglas box fitted with an interlock system to avoid electrical shock. The laser was focused onto the detection window of the capillary or the microchip and fluorescence was collected perpendicular to the incident beam by using a high numerical aperture microscope objective (Nikon) having 40× magnification, an NA of 0.85, and a 0.37 mm working distance. The background fluorescence and the scattered light were minimized by using a long-pass filter

and a variable slit. The fluorescence was collected by a photomultiplier tube (PMT; Hamamatsu, Japan) and the signal was amplified with a lock-in amplifier (Stanford Research Systems, Sunnyvale, CA, USA). The current output from the amplifier was recorded using a DAQ board in conjunction with a program written in Labview (National Instruments, Austin, TX, USA). All experiments were conducted at ambient temperatures.

Teflon-coated fused-silica capillaries (100 μm I.D.) were purchased from Polymicro Technologies (Phoenix, AZ, USA). DB-WAX capillaries (100 μm I.D.) for CE experiments were obtained from J & W Scientific (Folsom, CA, USA). Glass chips with a single T-injector design were fabricated in the laboratory. Photomask layout was performed using AutoCAD 2000 (Autodesk, San Rafael, CA, USA) and the generated file was converted to GDS format. The photomask was manufactured by Photo Sciences (Torrance, CA, USA). Schott D263 glass wafers were purchased from S. I. Howard Glass (Worcester, MA, USA). A Cooke (Cooke Vacuum Products, Norwalk, CT, USA) sputtering system was used to deposit the metal etch mask. A Karl Suss (Karl Suss America, Waterbury Center, VA, USA) MA6 contact mask aligner was used for photolithography. The microchannel dimensions were 25 μm deep and 50 μm wide; the separation channel length was 8.0 cm and the injection arms were 1.0 cm each.

2.2. Chemicals

High-purity potassium phosphate, thiourea and acetonitrile were used as received from Aldrich (Milwaukee, WI, USA). Sodium tetraborate was obtained from Sigma (St Louis, MO, USA). Napthalene-2,3-dicarboxaldehyde (NDA) and potassium cyanide were purchased from Molecular Probes (Eugene, OR, USA). All phenylthiohydantoin (PTH) amino acids and peptides were purchased from Sigma. Water was purified with an Ultra-Pure water system from Millipore (Milford, MA, USA). (Acrylamidomethyl)cellulose acetate butyrate was obtained from Aldrich and used as received. Other acrylate monomers were obtained and purified as previously described [24]. OCG 825 photoresist and OCG 934 developer were obtained from Arch (Columbus, OH, USA). Chrome etch was purchased from Microchrome Technologies (San Jose, CA, USA). High purity sulfuric acid and hydrofluoric acid were obtained from Ashland (Norwalk, CT, USA), and acetone and ammonium hydroxide were purchased from General Chemical (Parsippany, NJ).

2.3. Polymer stationary phases

Prior to in situ polymerization, the walls of capillaries and microchannels were silanized to ensure covalent attachment of the polymer to the substrate; this pretreatment has been previously described [24]. Both positively- and negatively-charged porous polymer monoliths containing butyl (C_4) and lauryl (C_{12}) groups were prepared according to a previously described procedure [24]. In the lauryl material, lauryl acrylate replaced 10% of the butyl monomer. The cellulose material was prepared from monomers in the following percentages: 1% (acrylamidomethyl)cellulose acetate butyrate, 10% tetrahydrofurfuryl (THF) acrylate, 1% [2-(acryloyloxy)ethyl]trimethylammonium methylsulfate, 58% butyl acrylate, 30% 1,3-butanediol diacrylate. The glass capillaries were pretreated to ensure adhesion of the polymer monoliths to the wall. For the positive material, a positive pretreatment solution was used to reverse the EOF as well as to promote adhesion.

2.4. CEC experiments

The packed capillary was electrokinetically conditioned using acetonitrile–5 m*M* Tris buffer pH 8 (80:20, v/v) or acetonitrile–25 m*M* phosphate buffer pH 2.8 (80:20, v/v) to remove residual monomeric materials prior to use. A detection window in the polymer was formed by exposure to 214 nm light from a UV light source.

For isocratic CEC separations of PTH-labeled amino acids using UV detection, negatively-charged butyl or lauryl monoliths (functionalized with sulfonic acid groups) were employed as stationary phases. The mobile phase was prepared by mixing the appropriate percentage of acetonitrile (by volume) in 25 m*M* phosphate solution pH 7.3 and was degassed by ultrasonication prior to use. The capillary was conditioned in the running buffer for approximately 1 h. Stock solutions of individual

PTH–amino acids were prepared in water and acetonitrile and sample solutions were diluted appropriately with buffer solution to attain final amino acid concentrations of 10^{-4} to 10^{-3} *M*. Thiourea (2.5 m*M*) was added to each sample mixture as the unretained marker. Amino acid samples were injected electrokinetically at the anode for 5 s at 2 kV and separations were performed at constant field strengths of 150–300 V/cm.

For isocratic CEC separations of native peptides using UV detection, positively-charged butyl monoliths (containing quaternary ammonium moieties) were used as stationary phases. The mobile phase (acetonitrile–12.5 m*M* phosphate buffer pH 2.8; 30:70, v/v) was degassed before use. The packed capillary was conditioned in this running buffer for 1 h. Peptide stock solutions (10^{-3} *M*) were prepared in water and final peptide samples of approximately 10^{-5} *M* were made by diluting with the running buffer. Peptide samples were electrokinetically injected at the cathode for 5 s at 1.5 kV and separated at constant field strengths of 90–200 V/cm.

For isocratic CEC separations of NDA-labeled amino acids using LIF detection, negatively-charged lauryl monoliths (functionalized with sulfonic acid groups) were employed as stationary phases. The mobile phase was prepared by mixing the appropriate percentage of acetonitrile (by volume) in 25 m*M* phosphate solution pH 7.2 and was degassed prior to use. The packed capillary was conditioned in the running buffer for approximately 1 h. Stock solutions of amino acids were prepared in water and working solutions of 0.3 m*M* were prepared by diluting in 50 m*M* borate buffer pH 9.5. Derivatization was carried out by adding aliquots of 40 μl of 4.8 m*M* KCN and 40 μl of 2.4 m*M* NDA to the 0.3 m*M* amino acid solution. The solutions were diluted with the run buffer to obtain final concentrations of 10^{-8} *M*. Amino acid samples were injected electrokinetically at the anode for 2 s at 4 kV and separations were performed at constant field strengths of 200 V/cm.

For on-chip electrochromatographic separations of peptides, negatively-charged lauryl monoliths (containing sulfonic acid groups) were cast in the microchannels. The mobile phase (acetonitrile–12.5 m*M* phosphate buffer pH 7.3; 35:65, v/v) was degassed before use. The packed channels were conditioned in this running buffer for 1 h. The peptides were labeled by adding a 40 μl aliquot of 0.3 m*M* peptide stock solution to 1 ml of 50 m*M* borate buffer pH 9.5, followed by aliquots of 40 μl of 4.8 m*M* KCN and 40 μl of 2.4 m*M* NDA. The solutions were diluted with the run buffer to obtain final concentrations of 10^{-6}– 10^{-7} *M*. Peptide samples were electrokinetically injected at the cathode for 30 s at 1.0 kV and separated at a constant field strength of 1200 V/cm. LIF was employed as the means of detection. An algorithm developed in-house was used for background subtraction and smoothing for all chromatographic data.

2.5. CE experiments

Unpacked, coated DB-WAX capillaries were used in order to eliminate EOF at the inner walls. The mobile phase (acetonitrile–12.5 m*M* phosphate buffer pH 2.8; 30:70, v/v) was degassed before use. Peptide sample solutions of approximately 10^{-5} *M* were hydrodynamically injected at the cathode for 10 s and separated at constant field strengths of 90–200 V/cm.

2.6. Chip fabrication

Glass wafers were sputtered with chrome (200 nm) which served as the etch mask. A 1-μm-thick layer of OCG 825 positive photoresist was spin-coated and soft-baked (90°C, 5 min). After exposure, the photoresist was developed with OCG 934 developer and hard-baked (120°C, 30 min). Exposed chrome was etched with a commercially available chrome etch and the subsequently exposed glass was etched with 25% HF solution. The photoresist was removed with acetone and the chrome mask was etched as described. Holes (1.0 mm diameter) were drilled in glass cover plates. The etched wafers and cover plates were cleaned with H_2SO_4–H_2O_2 (3:1)(90°C) and NH_4OH–H_2O–H_2O_2 (1:5:1)(60°C), aligned for contacting, and once contacted were thermally bonded at 650°C.

3. Results and discussion

3.1. Porous polymer monoliths

Acrylate-based porous polymer monoliths de-

veloped in our laboratory possess several properties that make them well-suited as reversed-phase chromatographic media [24]. They are readily cured (5 min in capillaries, and 10–20 min in microchannels) by UV irradiation and do not require retaining frits since they are covalently attached to the substrate surface. They support EOF as cast without the need to flush with pressure. They can be made from a wide variety of monomers, enabling the charge and hydrophobicity of the stationary phase to be easily tuned. High efficiencies (>150 000 plates/m) have been routinely obtained in the CEC separations of polyaromatic hydrocarbons and neutral aromatics using negatively- and positively-charged materials with varying degrees of hydrophobicity [24]. In this work, the applicability of both negative and positive polymer monoliths in the CEC separation of charged analytes was investigated.

In the negatively-charged material used for amino acid separations, a sulfonic acid monomer is incorporated to support EOF and the linear alkyl acrylates serve as hydrophobic sites for chromatographic retention. Scanning electron miscroscope (SEM) micrographs indicate that the polymer nodule structure is identical in both butyl and lauryl materials [24]. In both monoliths, the peak pore diameter by porosimetry is approximately 1 μm and the surface area by BET analysis is 1–3 m^2/g [24]. Fig. 1a is a representative SEM micrograph of a negative lauryl monolith.

In the positively-charged porous polymer monoliths used for peptide separations, a tetraalkylammonium compound serves as the charged functionality. The polymer nodule structure is similar to that observed for the negatively-charged materials, as shown by SEM microscopy (Fig. 1b), and BET

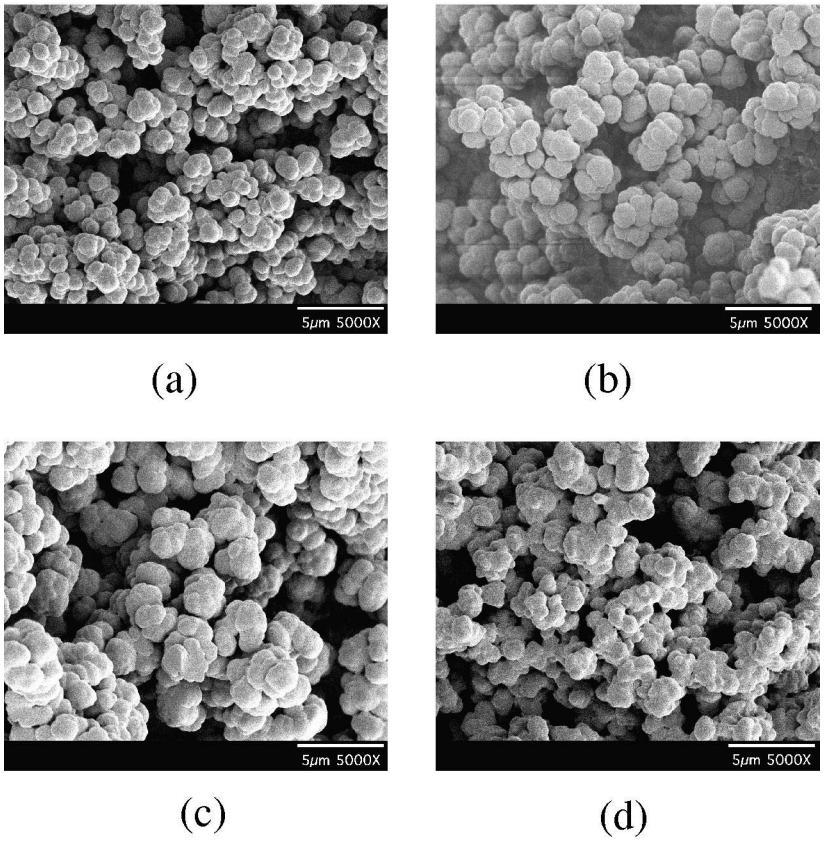

Fig. 1. SEM micrographs of methanol-extracted samples of (a) negatively-charged lauryl monolith, (b) positively-charged butyl monolith, (c) positively-charged butyl monolith with double the percentage (1%) of charged monomer, and (d) positively-charged butyl monolith with 1% cellulose.

surface area is 1–3 m^2/g. Unlike the negative monoliths, however, the positive materials exhibit a range of pore sizes between 1–2 μm without a distinct peak pore diameter (data not shown). In an effort to increase EOF, monoliths with twice the percentage of charged monomer were prepared with no significant effect on the morphology as depicted in Fig. 1c. Incorporation of 1% cellulose to the monomer mixture resulted in slightly smaller polymer nodule sizes (Fig. 1d). This is probably caused by solubility changes when including the more hydrophilic cellulose-based acrylate monomer in the growing monolith network.

3.2. Separation of PTH–amino acids

Peptide sequencing via Edman degradation renders the resultant PTH–amino acids neutral except for PTH–Arg, which is basic, and PTH–Asp and PTH–Glu, which are acidic. PTH–Thr exhibits two peaks, as observed by others [13]. The isocratic CEC separation of 20 PTH–amino acids was achieved using a lauryl (C_{12}) monolithic column containing highly acidic sulfonic acid groups. The mobile phase consisted of acetonitrile–25 m*M* phosphate buffer at pH 7.3; (40:60, v/v). As shown in Fig. 2, neutral hydrophilic amino acids elute first and all in this group but PTH–Gln and PTH–Asn are baseline-resolved. The neutral hydrophobic amino acids are significantly more retained and elute much later, as illustrated by PTH–Phe, PTH–Ile, PTH–Trp and PTH–Leu. PTH–Arg has an electrophoretic mobility in the same direction as EOF, whereas PTH–Asp and PTH–Glu have electrophoretic mobilities that oppose EOF. Since the acidic amino acids elute before PTH–Arg, we may conclude that the separation mechanism under these conditions is dominated by the hydrophobic interactions between the analytes and the monolithic stationary phase rather than by CZE. For the charged amino acids, coulombic interactions will also significantly influence retention. The PTH–Arg peak is broader and more asymmetric because it is also partly retained by electrostatic interactions with the negatively charged sulfonic acid groups of the monolith.

Separation efficiencies of up to 268 000 plates/m are obtained with the lauryl column as shown in Table 1. These values are comparable to those reported for conventional silica-based stationary phases used to separate neutral and acidic PTH–

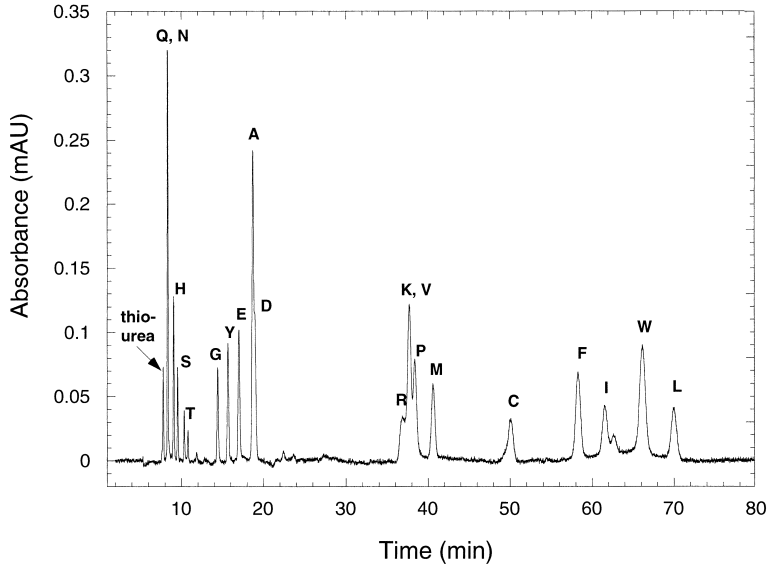

Fig. 2. Electrochromatographic separation of 20 PTH–amino acids on negatively-charged lauryl stationary phase in acetonitrile–25 m*M* phosphate pH 7.3 (40:60, v/v). UV detection at 214 nm. Field strength, 175 V/cm. Capillary: total length = 28.5 cm; length to detector = 17.5 cm; I.D. = 100 μm.

Table 1
Retention times, capacity factors and column efficiencies for the CEC separation of five PTH–amino acids using lauryl and butyl monolithic stationary phases

Amino acid	Lauryl			Butyl		
	t_r (min)	k'	N (plates/m)	t_r (min)	k'	N (plates/m)
PTH–Ala	18.7	1.41	176 000	10.6	1.07	127 000
PTH–Asp	18.9	– [a]	181 000	12.1	– [a]	134 000
PTH–Arg	36.8	– [a]	46 000 [b]	17.5	– [a]	14 000 [b]
PTH–Phe	58.3	6.50	238 000	24.8	3.84	120 000
PTH–Trp	66.2	7.51	268 000	27.0	4.28	116 000

[a] k′ cannot be calculated for charged analytes because retention depends on both chromatographic retention and electrophoretic mobility.
[b] The number of theoretical plates for the asymmetric PTH–Arg peak was obtained using the equation [22]: $N = 41.7\ (t_r/w_{0.1})^2/(A/B + 1.25)$.

amino acids by CEC. Efficiencies in the range of 60 000–213 000 plates/m have been achieved with 3 μm ODS-modified silica particles [13] while values of 176 000–530 000 plates/m have been obtained with 1.5 μm ODS-modified non-porous particles [11]. Mercury porosimetry indicates that the peak pore size of our acrylate-based monoliths is approximately 1 μm [24]. In phase-separated structures such as ours, we often observe a correlation between nodule size and pore size.

3.2.1. Effect of column hydrophobicity

The degree of column hydrophobicity has a significant effect on selectivity and on the quality of separations. Using a representative subset of PTH–amino acids, we compared the separation performance of a negative butyl (C_4) monolithic column to the negative lauryl (C_{12}) material. Under identical mobile phase conditions, column lengths and EOF velocities, we found that including 10% lauryl acrylate in the porous polymer monolith increases the retention times of all amino acids, and the most dramatic increase in capacity factor was observed for the most hydrophobic amino acids, PTH–Phe and PTH–Trp (Table 1). A concomitant increase in efficiencies was also noted and is probably due to differences in the morphologies of the butyl and lauryl materials. Resolution was generally greatly improved and well separated peaks were obtained for the PTH–Gln and PTH–His pair as well as for the group of amino acids consisting of PTH–Gly, PTH–Tyr, PTH–Glu and PTH–Ala, none of which could be baseline-resolved using the less hydrophobic column. However, while the PTH–Ala/PTH–Asp and PTH–Arg/PTH–Lys pairs could not be well-resolved on the lauryl column, they were well separated using the butyl column (data not shown). In addition, the elution order of PTH–Ala and PTH–Glu obtained with the lauryl column is reversed in the butyl stationary phase.

3.2.2. Effect of acetonitrile content

The volume percentage of acetonitrile in the mobile phase was found to dramatically affect the elution order of PTH–amino acids. A subset of amino acids was separated on a negative butyl (C_4) column using different volume ratios of acetonitrile–25 m*M* phosphate pH 7.3. Retention times were normalized with respect to the EOF to give a retention factor t_r/t_{eof}, which depends on both hydrophobic retention as well as electrophoresis (Fig. 3). In reversed-phase chromatography, separation is based on the partition of analytes between the hydrophobic stationary phase and the relatively polar mobile phase, hence increasing mobile phase polarity increases analyte retention. As shown in Fig. 3, the retention times of the neutral amino acids, particularly the most hydrophobic ones, increase as the acetonitrile content in the mobile phase is lowered.

For the charged amino acids, however, the separation mechanism is comprised of an electrophoretic component as well as a chromatographic one. It is possible to alter the balance of these two separation components to achieve the desired resolution and analysis speed by changing the mobile phase com-

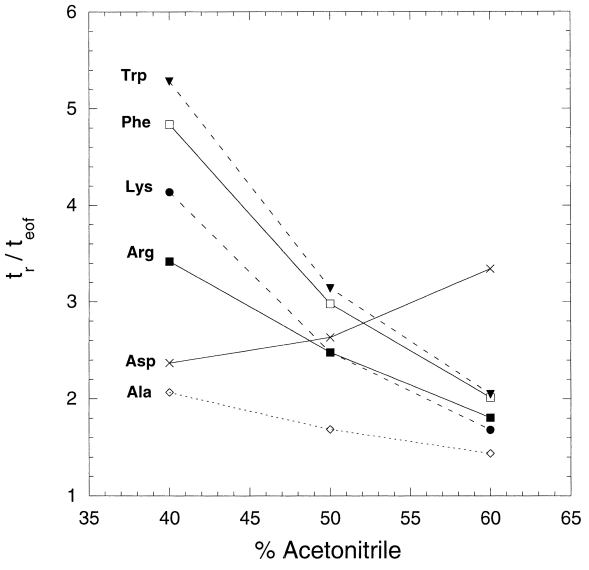

Fig. 3. Plot of normalized retention factor, t_r/t_{eof}, vs. percentage of acetonitrile for five PTH–amino acids separated on a negatively-charged butyl column. Capillary: total length = 25.0 cm; length to detector = 15.2 cm; I.D. = 100 μm.

position. At acetonitrile–25 m*M* phosphate (60:40), PTH–Ala elutes first, followed by PTH–Lys, positively-charged PTH–Arg, neutral hydrophobic PTH–Phe and PTH–Trp, and finally negatively-charged PTH–Asp. This elution order suggests that the amino acid separation is primarily due to the differences in electrophoretic mobility. CZE is still a major component in the separation mechanism at acetonitrile–25 m*M* phosphate buffer (50:50), where PTH–Arg elutes before PTH–Asp, but the degree of retention of the hydrophobic amino acids is significantly increased as indicated by the higher t_r/t_{eof} values. At a ratio of acetonitrile–25 m*M* phosphate (40:60), all the amino acids are significantly more retained except PTH–Asp, which now elutes before PTH–Arg, indicating that chromatographic interactions dominate the separation mechanism.

The acetonitrile content in the mobile phase also influences the EOF velocity, which is 6.81, 6.76, and 5.12 mm/s at 60%, 50% and 40% acetonitrile, respectively. By increasing the percentage of acetonitrile, the electrolyte concentration is concurrently decreased, which results in an increase in the zeta potential and hence a corresponding increase in the EOF velocity [25].

3.3. Separation of NDA-labeled amino acids

Significantly lower limits of detection can be achieved using LIF to detect amino acids derivatized with a fluorogenic reagent. NDA reacts with primary amines in the presence of cyanide to yield highly stable 1-cyano-2-alkylbenz[f]isoindole (CBI) adducts which exhibit high fluorescence quantum yields [26–30]. Upon NDA-labeling, most amino acids possess a single negative charge with the exception of NDA–Glu and NDA–Asp, which possess two negative charges, and NDA–Arg, which is neutral. Labeling difficulties are associated with Lys and Cys due to intramolecular fluorescence quenching [31], and Pro cannot be labeled with NDA because it does not possess a primary amine. Fig. 4 shows the isocratic CEC separation of 15 NDA-labeled amino acids (concentrations of 10^{-8} *M*) employing sensitive LIF detection and using a lauryl (C_{12}) monolith containing sulfonic acid groups and a mobile phase of acetonitrile–20 m*M* phosphate buffer at pH 7.2 (15:85, v/v). NDA–Glu and NDA–Asp could be separated (data not shown) on the same stationary phase using a mobile phase of acetonitrile–12.5 m*M* phosphate buffer at pH 7.2 (15:85, v/v) with retention times of 50.8 min and 58.4 min, respectively (a lower buffer concentration was necessary to achieve faster separations of these two doubly-nega-

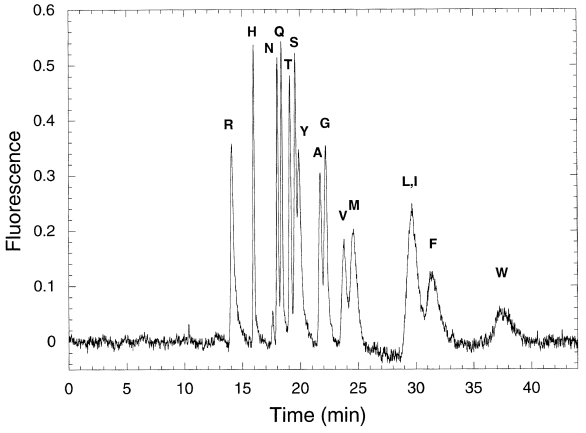

Fig. 4. Electrochromatographic separation of 15 NDA–amino acids on negatively-charged lauryl stationary phase in acetonitrile–20 m*M* phosphate pH 7.2 (15:85, v/v). LIF detection at 413 nm. Field strength, 200 V/cm. Capillary: total length = 33.0 cm; length to detector = 23.5 cm; I.D. = 100 μm.

tive species on the negatively charged stationary phase). Fourteen of the 15 NDA-labeled amino acids are well resolved with only NDA–Leu and NDA–Ile coeluting, and efficiencies in the range of 65 000–371 000 plates/m were obtained. The resolution of our NDA–amino acid separations compare favorably with those achieved using gradient elution HPLC–LIF on C_{18} stationary phases [27,28,30,32], demonstrating the applicability of both CEC and polymer monolithic stationary phases in the separation of charged analytes.

3.4. Separation of basic bioactive peptides

Separation of peptides by CEC requires consideration of the nature of the charged groups on the stationary phase and the pH of the mobile phase. Peptides possess a characteristic isoelectric point (p*I*) and so their net charge varies with the pH of the solution. If the p*I* values of the peptides are known, the pH of the mobile phase should be chosen so as to minimize the electrostatic attraction between most of the peptides and the stationary phase. This can be achieved by careful selection of a stationary phase and a mobile phase pH that will allow the peptides to have the same sign of charge as that of the chromatographic support. However, this leads to the peptides migrating electrophoretically in a direction opposite to the EOF, potentially slowing down their migration. Another factor to consider is the instability of siloxane bonds that link the monolith to the capillary wall at a pH of 8 or higher, thereby requiring separation to be performed at acidic or neutral pH. We selected eight bioactive peptides that had p*I* values ranging from 8.5–8.9 as model analytes for CEC that was performed at a pH of 2.8. This necessitates the use of a monolithic column containing basic groups such as quaternary ammonium in order to suppress electrostatic interactions between the net positively-charged peptides and the charged groups on the stationary phase. Researchers have traditionally obtained positively-charged supports by coating silica particles with silanes functionalized with an amine or quaternary amine but such coatings may be unstable [33] and the EOF is adversely affected by the residual negatively charged silanols [34].

Fig. 5 illustrates the isocratic CEC separation of

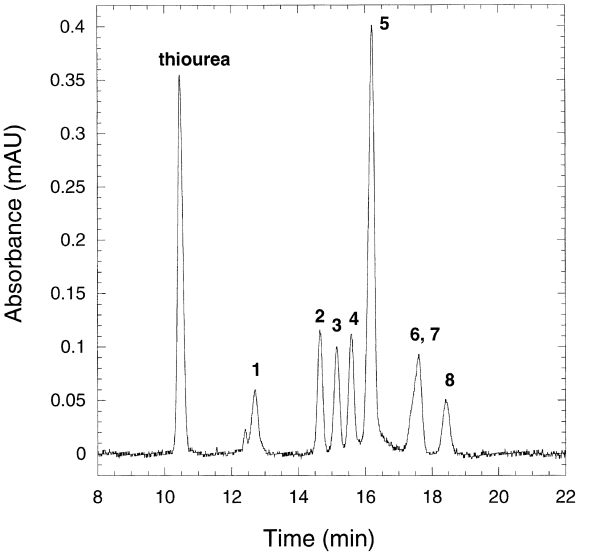

Fig. 5. Electrochromatographic separation of eight bioactive peptides on positively-charged butyl stationary phase incorporated with 0.5% charge in acetonitrile–12.5 m*M* phosphate pH 2.8 (30:70, v/v). UV detection at 214 nm. Field strength, 93 V/cm. Capillary: total length = 32.5 cm; length to detector = 18.5 cm; I.D. = 100 μm. The numbers labeling the peaks correspond to the designations in Table 2.

eight bioactive peptides using a monolithic butyl column containing quaternary ammonium groups (0.5%, w/w) and a mobile phase of acetonitrile–12.5 m*M* phosphate buffer at pH 2.8 (30:70, v/v) . All peptides are baseline resolved except for thymopentin (**6**) and splenopentin (**7**), which differ by only one CH_2 unit (Table 2). Column efficiencies range between 91 000–324 000 plates/m (Table 2), compared to the efficiency value of 43 000 plates/m reported for a peptide separation using a negatively-charged methacrylate-based monolithic stationary phase [8], and values of 32 000–44 000 plates/column, corresponding to 110 000–151 000 plates/m, reported for a CEC separation of four proteins using a positively-charged methacrylate-based monolithic column [7]. Increasing the field strength resulted in a faster EOF velocity and, accordingly, faster peptide elution times.

The peptides were separated by electrophoresis under identical conditions using an open and coated (to eliminate EOF) capillary in order to elucidate the separation mechanism. Only three poorly-resolved peaks were obtained by this method (data not

Table 2
Normalized retention factors and column efficiencies for the CEC separation of eight bioactive peptides using monolithic stationary phases of different compositions

Peptide	Name	Sequence	p*I*	0.5% charge		1% charge		1% charge + 1% cellulose	
				t_r/t_{eof}	*N* (plates/m)	t_r/t_{eof}	*N* (plates/m)	t_r/t_{eof}	*N* (plates/m)
1	Leu–Enkephalin–Lys	YGGFLK	8.59	1.21	92 000	1.25	99 000	1.26	116 000
2	Met–Enkephalin–Arg–Phe	YGGFMRF	8.75	1.40	284 000	1.48	108 000	1.49	213 000
3	α-Casein, fragment 90–95	RYLGYL	8.59	1.45	241 000	1.55	–	1.57	–
4	Met–Enkephalin–Lys	YGGFMK	8.59	1.49	324 000	1.55	–	1.57	–
5	β-Lipotropin, fragment 39–45	KKDSGPY	8.50	1.55	225 000	1.70	138 000	1.69	265 000
6	Thymopentin	RKDVY	8.59	1.68	–	1.87	171 000	1.87	330 000
7	Splenopentin	RKEVY	8.59	1.68	–	1.93	–	1.96	205 000
8	Kyotorphin	YR	8.75	1.76	177 000	1.93	–	1.91	274 000

shown). Leucine–enkephalin–lysine (**1**) and methionine–enkephalin–arginine–phenylalanine (**2**) co-elute to give the first peak, methionine–enkephalin–lysine (**4**) and β-lipotropin (fragment 39–45) (**5**) co-elute as the second peak, and the remaining peptides comprise the third peak.

Retention of peptides in CEC is expected to involve contributions from chromatographic interactions and electrophoretic mobilities of the solutes. In order to elucidate the relative importance of these two contributions, we have used empirical models to calculate retention and migration times for the peptides. A theoretical retention order for small peptides composed of less than 15 amino acid residues may be predicted from a summation of hydrophobicity constants associated with the constituent amino acids for each peptide [35]:

$$t_{Ri} = A \Sigma D_j n_{ij} + B \quad (1)$$

where t_{Ri} is the peptide retention time peptide i, D_j is the retention constant of amino acid j, n_{ij} is the number of amino acid residues j in peptide i, and *A* and *B* are constants determined from data fitting. We used the hydrophobic retention constants calculated by Sasagawa and Teller, which are based on retention times measured on a C_{18} column [35]. Normalization was performed for the retention order so that the least retained peptide corresponds to a retention value of 0 while the most retained peptide corresponds to a retention value of 1. For each retention order, normalization was carried out using (*X* − minimum value)/(maximum value − minimum value), where *X* is the value obtained for peptide X, and minimum and maximum values are the values obtained for the least retained peptide and the most retained peptide, respectively. Fig. 4 clearly shows that the predicted elution order based on this model differs remarkably from what is actually observed, indicating that CZE must play a significant role in the CEC separation.

Furthermore, Fig. 6 illustrates that the elution order follows closely to the order predicted for electrophoretic migration by the ratio $q/M_r^{2/3}$, where

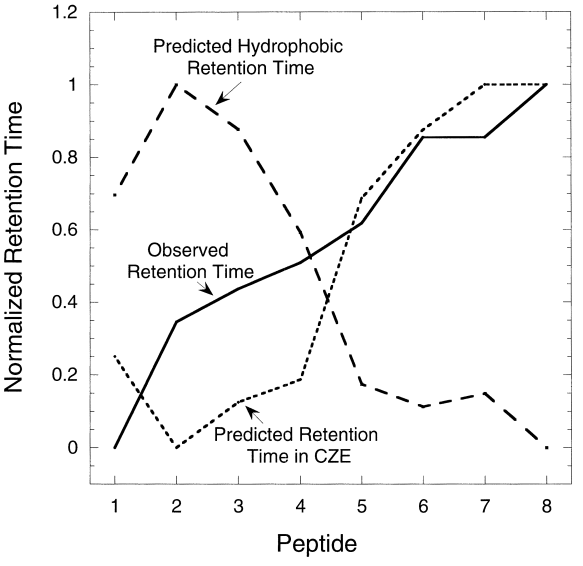

Fig. 6. Plot comparing the observed peptide retention order with the predicted retention orders based on amino acid hydrophobicity constants and calculated electrophoretic factors. The numbers labeling the peptide *x*-axis correspond to the peptide designations in Table 2. The equations used to generate the data are discussed in the text.

q is the net charge of the peptide calculated using the Henderson–Hasselbach equation [36] and adjusted pK_a values for associated amino acids [37], and M_r is the molecular mass [37,38]. The predicted migration order was normalized as described above for the predicted retention order. The correlation between this ratio and electrophoretic mobility has been demonstrated before in the CZE of peptides [37,39,40]. It therefore appears that electrophoretic migration largely determines the peptide elution order but interactions with the stationary phase provide additional selectivity.

The effect of changing stationary phase properties was also investigated. Increasing the surface charge of the monolith resulted in a small increase in the EOF velocity and peptides eluted slightly faster accordingly but with some loss in resolution (Fig. 7). The copolymerization of cellulose ester acrylate, which is used in chiral stationary phases [41,42], improves resolution as shown in Fig. 8. Presumably the incorporation of the polysaccharide to the monolith allows for polar interactions between the cellulose ester and the peptides [42], enabling enhanced resolution of individual peptide peaks. The polymer monoliths can therefore be tuned for selectivity, providing a useful means of separating different sets of peptides. Table 2 compares the normalized retention factors and column efficiencies obtained from the separation of peptides **1**–**8** using the different monolithic stationary phases.

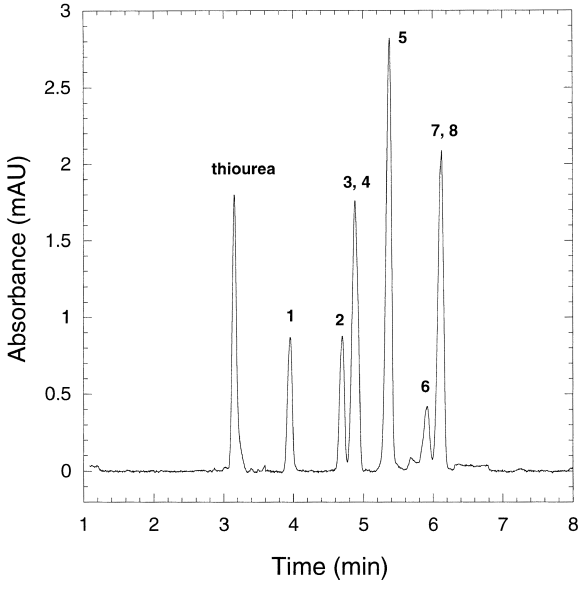

Fig. 7. Electrochromatographic separation of eight bioactive peptides on positively-charged butyl stationary phase incorporated with 1% charge in acetonitrile–12.5 m*M* phosphate pH 2.8 (30:70, v/v). UV detection at 214 nm. Field strength, 200 V/cm. The numbers labeling the peaks correspond to the designations in Table 2.

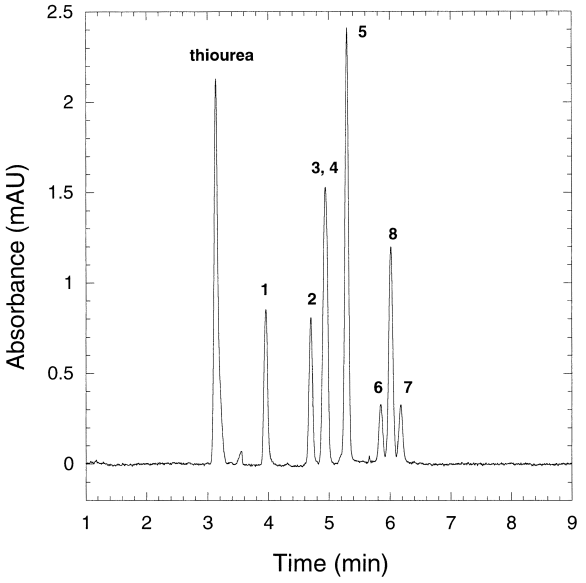

Fig. 8. Electrochromatographic separation of eight bioactive peptides on positively-charged butyl stationary phase incorporated with 1% charge and 1% cellulose ester in acetonitrile–12.5 m*M* phosphate pH 2.8 (30:70, v/v). UV detection at 214 nm. Field strength, 200 V/cm. The numbers labeling the peaks correspond to the designations in Table 2.

3.5. On-chip CEC separation of bioactive peptides

Our porous polymer monoliths were designed for rapid and facile placement in the channels of glass-based microfluidic devices, obviating the need for frits and the difficulties of packing silica beads. Pretreatment of the substrate surface ensures that the polymer is covalently attached to the substrate, and polymerization under UV irradiation is between 10 and 20 min in microchannels. The material supports sufficient EOF as cast and no pressure is required for purging. To demonstrate the applicability of polymer monoliths for chip-based CEC separations, Fig. 9 shows a preliminary on-chip electrochromatographic

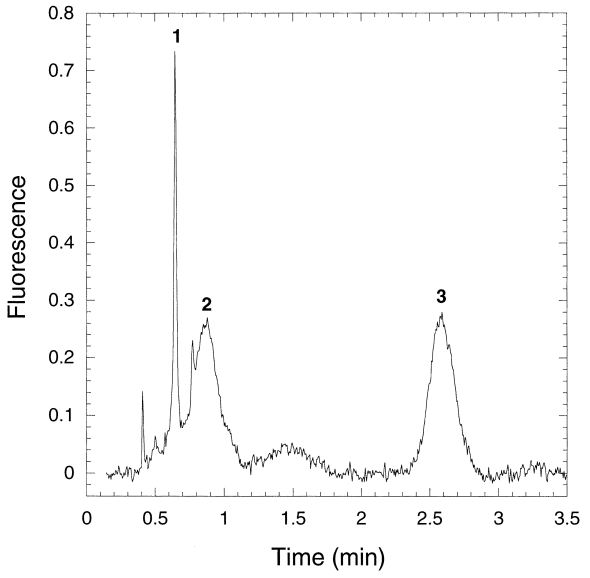

Fig. 9. Electrochromatographic separation of three NDA-labeled bioactive peptides on negatively-charged lauryl monolithic stationary phase cast in a glass chip. LIF detection at 413 nm. Field strength, 1200 V/cm. Mobile phase: acetonitrile–12.5 m*M* phosphate pH 7.0 (35:65, v/v). Microchannel dimensions: 25 μm deep, 50 μm wide; separation channel length, 8.0 cm; injection arms, 1.0 cm each; length to detector, 7.0 cm. Peaks: (1) papain inhibitor, GGYR, (2) α-casein (fragment 90–95), RYLGYL, (3) Ile–angiotensin III, RVYIHPI.

separation of three NDA-labeled bioactive peptides using a monolithic lauryl column containing sulfonic acid groups, a mobile phase of acetonitrile–12.5 m*M* phosphate buffer at pH 7.0 (35:65, v/v), and LIF detection. These peptides contain an arginine residue, which counters the negative charge on the C-terminal carboxyl group that remains after NDA-labeling at a neutral pH. The peptides are baseline-resolved and the column efficiencies are 83 000, 1500 and 11 000 plates/m for papain inhibitor (**1**), α-casein (fragment 90–95) (**2**) and Ile–angiotensin III (**3**), respectively. Although the peptides should be net neutral at this pH, we believe that the broad peaks exhibited by α-casein (fragment 90–95) (**2**) and Ile–angiotensin III (**3**) may be due to electrostatic interactions between the positive charge localized at the N-terminal arginine residue and the negatively-charged stationary phase. In contrast, the positive and negative charges in papain inhibitor (**1**) are both located at the C-terminal arginine residue, allowing more effective charge cancellation.

3.6. Column stability and reproducibility

The monolithic columns were very stable over time and could be used for months without any noticeable degradation in separation efficiency. The single column run-to-run percent standard variation was 2.1% ($n=9$) for the negatively charged lauryl material (based on the retention time for PTH–Glu) and 3.8% ($n=8$) for the positively charged butyl monoliths (based on the retention time for kyotorphin). The column-to-column variation was 10% ($n=3$) and 14% ($n=3$) for the negatively- and positively-charged monoliths, respectively.

4. Conclusions

Acrylate-based porous polymer monoliths have been used as reversed-phase chromatography media for highly efficient and reproducible CEC separations of both neutral and charged PTH–amino acids, NDA-labeled amino acids and bioactive peptides in capillaries and in chips. The monoliths are tunable for charge and hydrophobicity, and incorporation of cellulose esters leads to further changes in selectivity. The separation mechanism of amino acids is strongly influenced by the degree of column hydrophobicity and the mobile phase composition. In CEC of peptides, both electrophoresis and chromatographic retention contribute to speed and selectivity. The present work demonstrates that CEC using porous polymer monolith stationary phases is a powerful technique for separation of charged analytes of biological importance.

Acknowledgements

The authors thank Dr. Issac Shokair for developing the software for data smoothing and background subtraction, George Sartor for help in microfabrication, and Jim Brennan and Gary Hux for technical assistance. This work was supported by the Laboratory Directed Research and Development program of Sandia National Laboratories. Sandia is a multiprog-

ram laboratory operated by Sandia Corporation, a Lockheed Martin Company, for the United States Department of Energy under contract DE-AC04-94AL85000.

References

[1] C.K. Larive, S.M. Lunte, M. Zhong, M.D. Perkins, G.S. Wilson, G. Gokulrangan, T. Williams, F. Afroz, C. Schöneich, T.S. Derrick, C.R. Middaugh, S. Bogdanowich-Knipp, Anal. Chem. 71 (1999) 389R.
[2] K. Stulík, V. Pacáková, J. Suchánková, H.A. Claessens, Anal. Chim. Acta 352 (1997) 1.
[3] J.-T. Wu, P. Huang, M.X. Li, M.G. Qian, D.M. Lubman, Anal. Chem. 69 (1997) 320.
[4] C. Ericson, S. Hjertén, Anal. Chem. 71 (1999) 1621.
[5] A. Apffel, H. Yin, W.S. Hancock, D. McManigill, J. Frenz, S.-L. Wu, J. Chromatogr. A 832 (1999) 149.
[6] J.-T. Wu, P. Huang, M.X. Li, D.M. Lubman, Anal. Chem. 69 (1997) 2908.
[7] S. Zhang, X. Huang, J. Zhang, Cs. Horvath, J. Chromatogr. A 887 (2000) 465.
[8] C. Yu, F. Svec, J.M.J. Fréchet, Electrophoresis 21 (2000) 120.
[9] B. He, J. Ji, F.E. Regnier, J. Chromatogr. A 853 (1999) 257.
[10] G. Choudhary, Cs. Horváth, J.F. Banks, J. Chromatogr. A 828 (1998) 469.
[11] R.M. Seifar, J.C. Kraak, H. Poppe, W.T. Kok, J. Chromatogr. A 832 (1999) 133.
[12] C.G. Huber, G. Choudhary, Cs. Horvath, Anal. Chem. 69 (1997) 4429.
[13] M. Qi, X.-F. Li, C. Stathakis, N.J. Dovichi, J. Chromatogr. A 853 (1999) 131.
[14] C. Ericson, J. Holm, T. Ericson, S. Hjertén, Anal. Chem. 72 (2000) 81.
[15] E.C. Peters, M. Petro, F. Svec, J.M.J. Fréchet, Anal. Chem. 69 (1997) 3646.
[16] E.C. Peters, M. Petro, F. Svec, J.M.J. Fréchet, Anal. Chem. 70 (1998) 2296.
[17] E.C. Peters, M. Petro, F. Svec, J.M.J. Fréchet, Anal. Chem. 70 (1998) 2288.
[18] F. Svec, J.M.J. Fréchet, Anal. Chem. 64 (1992) 820.
[19] F. Svec, J.M.J. Fréchet, Ind. Eng. Chem. Res. 38 (1999) 34.
[20] F. Svec, E.C. Peters, D. Sykora, C. Yu, J.M.J. Fréchet, J. High Resol. Chromatogr. 23 (2000) 3.
[21] A. Palm, M.V. Novotny, Anal. Chem. 69 (1997) 4499.
[22] X. Huang, J. Zhang, Cs. Horváth, J. Chromatogr. A 858 (1999) 91.
[23] I. Gusev, X. Huang, Cs. Horváth, J. Chromatogr. A 855 (1999) 273.
[24] S.M. Ngola, Y. Fintschenko, W.-Y. Choi, T.J. Shepodd, Anal. Chem. 73 (2001) 849.
[25] L.A. Colon, Y. Guo, A. Fermier, Anal. Chem. 69 (1997) 461A.
[26] R.G. Carlson, K. Srinivasachar, R.S. Givens, B.K. Matuszewski, J. Org. Chem. 51 (1986) 3978.
[27] M.C. Roach, M.D. Harmony, Anal. Chem. 59 (1987) 411.
[28] P. de Montigny, J.F. Stobaugh, R.S. Givens, R.G. Carlson, K. Srinivasachar, L.A. Sternson, T. Higuchi, Anal. Chem. 59 (1987) 1096.
[29] B. Matuszewski, R. Givens, K. Srinivasachar, R. Carlson, T. Higuchi, Anal. Chem. 59 (1987) 1102.
[30] F. Lai, T. Sheehan, Biotechniques 14 (1993) 642.
[31] M. Oates, J. Jorgenson, Anal. Chem. 61 (1989) 432.
[32] S.S. Yang, I. Smetena, Chromatographia 37 (1993) 593.
[33] A. Cifuentes, M.A. Rodríguez, F.J. García-Montelongo, J. Chromatogr. A 742 (1996) 257.
[34] D. Corradini, J. Chromatogr. B 699 (1997) 221.
[35] T. Sasagawa, D.C. Teller, in: W.S. Hancock (Ed.), CRC Handbook of HPLC for the Separation of Amino Acids, Peptides, and Proteins, Vol. 2, CRC Press, Boca Raton, FL, 1984, p. 53.
[36] D.C. Harris, Quantitative Chemical Analysis, Freeman, New York, 1999.
[37] E.C. Rickard, M.M. Strohl, R.G. Nielsen, Anal. Biochem. 197 (1991) 197.
[38] S. Fu, C.A. Lucy, Anal. Chem. 70 (1998) 173.
[39] N. Adamson, P.F. Riley, E.C. Reynolds, J. Chromatogr. 646 (1993) 391.
[40] H.G. Lee, D.M. Desiderio, J. Chromatogr. A 666 (1994) 271.
[41] A. Ishikawa, T. Shibata, J. Liq. Chromatogr. 16 (1993) 859.
[42] Y. Okamoto, E. Yashima, Angew. Chem. Int. Ed. Engl. 37 (1998) 1020.